INSTITUT D'AERONOMIE SPATIALE DE BELGIQUE

3 - Avenue Circulaire
B - 1180 BRUXELLES

AERONOMICA ACTA

A - N° 299 - 1985

Dynamical plasmapause positions during the july 29-31, 1977, storm period : a comparison of observations and time dependent model calculations

by

Y. CORCUFF, P. CORCUFF and J. LEMAIRE

BELGISCH INSTITUUT VOOR RUIMTE-AERONOMIE

3 - Ringlaan
B - 1180 BRUSSEL

FOREWORD

This work has been presented August 17th, 1983 at the symposium "Role of Ionospheric Plasma in the Plasmasphere and Magnetosphere" which has been held in Hamburg during the XVIIIth Meeting of IAGA. It will be published in "ANNALES GEOPHYSICAE".

AVANT-PROPOS

Ce travail a été présenté le17 août 1983 au symposium "Role of Ionospheric Plasma in the Plasmasphere and Magnetosphere" qui s'est tenu à Hamburg, lors de la XVIIIe Assemblée Générale IUGG de l'IAGA. Ce travail sera publié dans "ANNALES GEOPHYSICAE".

VOORWOORD

Dit werk werd op 17 augustus 1983 voorgedragen bij het symposium "Role of Ionospheric Plasma in the Plasmasphere and Magnetosphere" gehouden te Hamburg tijdens de XVIIIe IAGA vergadering. Dit werk zal uitgegeven worden in "ANNALES GEOPHYSICAE".

VORWORT

Diese Arbeit ist am 17 August 1983 zum symposium "Role of Ionospheric Plasma in the Plasmasphere and Magnetosphere" das in Hamburg während des IAGA meeting, mitgeteilt worden. Die Arbeit wird in "ANNALES GEOPHYSICAE" herausgegeben werden.

DYNAMICAL PLASMAPAUSE POSITIONS DURING THE JULY 29-31, 1977, STORM PERIOD : A COMPARISON OF OBSERVATIONS AND TIME DEPENDENT MODEL CALCULATIONS

by

Y. CORCUFF*, P. CORCUFF* and J. LEMAIRE**

Abstract

The theory for the formation of the plasmapause proposed by Lemaire (1974, 1975) takes into account the mechanism of plasma interchange motion. In the framework of this theory, which has been illustrated by Lemaire and Kowalkowski (1981) using McIlwain's stationary electric field model E3H, plasma density holes always tend to drift toward an asymptotic trajectory identified as the plasmapause. In the present article, we extend the application of this numerical method to non-stationary E-field models to test the theory during a magnetic storm situation.

The temporal evolution of the plasmapause boundary is studied over a period of three and a half days covering the successive substorm events of July 29 and July 30, 1977. The equatorial plasmapause position in different local time sectors is first calculated as a function of universal time using electric field distributions derived from the models of Volland-Stern and McIlwain, with similar variation of the electric field intensity as a function of the K_p index.

---

* Laboratoire de Physique de la Haute Atmosphère, Université de Poitiers, Le Deffend, Mignaloux-Beauvoir, F-86800 Saint Julien L'Ars, France.

** Institut d'Aéronomie Spatiale de Belgique, 3 avenue Circulaire, B-1180 Bruxelles, Belgique.

Model predictions are then compared with experimental data deduced from a large number of whistlers received at Kerguelen and at General Belgrano. In-situ electron density measurements made on board the GEOS-1 satellite, and estimates of low-altitude plasmapause boundaries deduced by Fennell et al. (1982) from S3-3 satellite data are also used for this study.

From the comparison of the observations and theoretical model calculations, we infer that when the mechanism of plasma interchange motion is taken into account the calculated positions of the plasmapause fit the observations better than in the case of the classical MHD approximation.

The time dependent E3H and Volland-Stern's electric field models respectively describe satisfactorily a number of features which are observed. Some of the observations presented can be interpreted in favor of both E-field models. The discrepancies found between the observations and the numerical simulations can be used to correct the empirical E-field models used in model calculations of the plasmpause positions.

Résumé

On a déterminé l'évolution des positions de la plasmapause pendant la période des sous-orages magnétiques survenus les 29 et 30 juillet 1977. Les positions équatoriales de la plasmapause ont été calculées en fonction du temps universel en utilisant deux types différents de modèles de champs électriques dépendant de la valeur de l'indice d'activité géomagnétique K_p. Ces deux distributions sont déduites respectivement du modèle de Volland-Stern et de celui de McIlwain. Pour chacunes de ces deux distributions de champs électriques on a effectué le calcul des positions de la plasmapause avec et sans tenir compte du mécanisme d'instabilité d'échange proposé par Lemaire (1975) pour expliquer la formation de la plasmapause.

On montre notamment que la définition classique de la plasmapause conduit en général à des résultats arbitraires qui ne sont pas indépendant des conditions initiales. Seule la méthode de calcul basée sur le mécanisme d'instabilité d'échange donne des positions de plasmapause qui sont indépendantes des conditions initiales.

Les positions théoriques de la plasmapause sont comparées avec des valeurs expérimentales déduites d'un grand nombre d'observations de sifflements magnétosphériques recueillis aux stations de Kerguelen et de General Belgrano. Des mesures de densités électroniques réalisées à l'aide des satellites GEOS-1 et S3-3 ont également été utilisées dans notre étude.

De la comparaison des observations et des résultats théoriques on peut conclure que le mécanisme d'instabilité d'échange est important dans le processus de formation de la plasmapause. Nous montrons également que de telles comparaisons entre les positions théoriques et expérimentales de la plasmapause permettent d'améliorer les modèles de distribution des champs électriques de la magnétosphère.

Samenvatting

Men heeft de evolutie van de plaatsen van de plasmapauze bepaald gedurende de periode van de magnetische deelstormen die zich voordeden op 29 en 30 juli 1977. De equatoriale plaatsen van de plasmapauze werden berekend in functie van de universele tijd en gebruik makend van twee verschillende soorten modellen van elektrisch veld die afhankelijk zijn van de waarde van de geomagnetische activiteitsindex K_p. De twee verdelingen worden respectievelijk afgeleid van het model van Volland-Stern en dat van McIlwain. Voor elk van deze twee elektrische veldverdelingen werden de plaatsen van de plasmapauze berekend om de vorming van de plasmapauze uit te leggen. De ene keer werd hierbij rekening gehouden met het onstabiliteitsuitwisselingsmechanisme voorgesteld door Lemaire (1975); de andere keer werd er geen rekening mee gehouden.

Men toont vooral dat de klassieke definitie van de plasmapauze gewoonlijk leidt tot arbitraire resultaten die niet onafhankelijk zijn van de begintoestanden. Alleen de berekeningsmethode die gebaseerd is op het onstabiliteitsuitwisselingsmechanisme geeft de plaatsen van de plasmapauze die afhankelijk zijn van de begintoestanden.

De theoretische plaatsen van de plasmapauze worden vergeleken met experimentele waarden afgeleid van een groot aantal magnetosferische fluiter-waarnemingen verzameld in de stations van Kerguelen en General Belgrano. Metingen van elektronendichtheid, verricht met behulp van de satellieten GEOS-1 en S3-3, werden eveneens in onze studie gebruikt.

Van de vergelijking van de waarnemingen en de theoretische resultaten kunnen wij besluiten dat het onstabiliteitsuitwisselingsmechanisme een belangrijke factor is bij de vorming van de plasma-

pauze. Wij tonen eveneens aan dat dergelijke vergelijkingen tussen de theoretische en experimentele plaatsen van de plasmapauze toelaten de verdelingsmodellen van de elektrische velden van de magnetosfeer te verbeteren.

Zusammenfassung

Man hat die Evolution der Plätze der Plasmapause bestimmt während der Periode der magnetischen Teilstürmer am 29 und 30 Juli 1977. Die Äquatorialplätze der Plasmapause wurden berechnet mit Rücksicht auf der universellen Zeit und zwei verschiedene Sorten Modellen von elektrisches Feld gebrauchend, abhängig vom Wert der geomagnetischen Aktivitätsindex K_p. Die zwei Verteilungen werden respektive abgeleiteit vom Modell Volland-Stern und McIlwain. Für jede von diesen zwei Verteilungen von elektrisches Feld werden die Plätze der Plasmapause berechnet um die Formung der Plasmapause zu erklären. Einmal wurde gerechnet mit dem Unstabilität-Austauschmechanismus vorgestellt vom Lemaire (1975); ein anderes Mal hatte man nicht mit dem Mechanismus gerechnet.

Man zeigt besonders dass die klassische Definition der Plasmapause gewöhnlich führt zu willkürliche Resultaten die nicht unabhängig sind von den Anfangszustanden. Nur die Berechnungsmethode die sich basiert auf dem Unstabilität-Austauschmechanismus gibt die Plätze der Plasmapause die abhängig sind von den Anfangszustanden.

Die theoretische Plätze der Plasmapause werden verglichen mit Experimentalwerten abgeleiteit von vielen magnetosferischen Pfeifgeräuschebeobachtungen gesammelt in den Stationen Kerguelens und General Belgranos. Messungen von Elektronendichtigkeit, getan mit der Hilfe von den Satelliten GEOS-1 und S3-3, wurden auch in unserer Studie benützt.

Von der Vergleichung der Beobachtungen und der theoretischen Resultaten, können wir uns entschliessen dass das Unstabilität-Austauschmechanismus ein wichtiger Faktor ist bei der Formung der Plasmapause. Wir zeigen auch dass solche Vergleichungen,

zwischen den theoretischen und experimentellen Plätzen der Plasmapause, zulassen die Verteilungsmodellen der elektrischen Felden der Magnetosphäre zu verbessern.

1. INTRODUCTION

Two theories have been proposed in the past to explain the plasma density gradients associated with the plasmapause. In both of them, the magnetospheric plasma motion is dominated by the large scale convection velocity $\underline{V} = (\underline{E} \times \underline{B})/B^2$ where $\underline{B}$ is the geomagnetic field and $\underline{E}$ the perpendicular electric field : the sum of the corotational and solar wind induced electric fields. The latter, for which many different models have been proposed (see, for instance, reviews by Lemaire (1975) and by Stern (1977)), has a dominant component directed from dawn towards dusk across the magnetosphere.

In the simple MHD theory of the plasmapause formation, it is assumed that the ionosphere is a very good conductor of electricity, and consequently that the integrated Pedersen conductivity of all magnetic field lines, as well as the parallel electric conductivity, are both infinitely large. As a result the perpendicular electric field inside any magnetospheric plasma element must be identical to the large scale background (external) electric field. The streamlines of plasma flux-tubes are then parallel to the equipotential surfaces corresponding to the externally imposed electric field.

According to this approach, the plasmapause is considered to be the last closed equipotential surface of the electric field which has often been purposely tailored to fit the observations (Brice 1967). In the analytical and classical model of Kavanagh et al. (1968), this equi-potential coincides with the boundary between plasma flux-tubes that drift indefinitely along closed streamlines around the Earth, and flux tubes that are periodically emptied when they drift to the magnetopause as a result of MHD convection (Nishida, 1966). In this model the solar wind induced electric field is assumed to have a uniform intensity E_o directed from dawn to dusk; the last closed equipotential defines a

tear-drop shaped plasmapause and is characterized by a stagnation point whose position at 1800 LT depends on E_o.

However, in empirical electric field models like McIlwain's E3H model (1974), the last closed equipotential extends to the magnetopause far beyond the actual position of the observed plasmapause in the dusk sector (Carpenter, 1966). This and other considerations have led Lemaire (1975) and Lemaire and Kowalkowski (1981) to propose a different physical mechanism for the formation of the plasmapause.

This alternative mechanism leads to the natural formation of a "knee" in the equatorial plasma density distribution even for the simple corotation electric field distribution devoid of any stagnation point (or any other mathematical singularity), and for which the last closed equipotential extends also to the magnetopause as in the case of McIlwain's E3H model. According to the mechanism proposed by Lemaire, the formation of the plasmapause is a consequence of interchange motion of plasma elements in the fields of gravitational and "centrifugal" forces.

In order to achieve significant interchange velocities, the values of the Pedersen conductivity must be low and comparable to those existing in the nightside ionosphere. Indeed, the interchange velocity $\underline{u}$, for a plasma element with density smaller or larger than the background density, is inversely proportional to the integrated Pedersen conductivity (Lemaire, 1975); $\underline{u}$ is also proportional to the difference in densities between the inside and the outside of a plasma irregularity. Near midnight, this interchange velocity can become as large as 30 per cent of the convection velocity $\underline{V}$ of the background plasma as determined from the external E-field intensity. The interchange velocity becomes equal to zero where the gravitational and centrifugal accelerations balance each other. Beyond this limit any plasma density excess is peeled off from the plasmasphere, and ejected

by the "centrifugal force". On the contrary, as shown in figure 1, a plasma hole whose density is smaller than the background density, and which is released inside the plasmasphere, will spiral outward until it reaches a stable asymptotic trajectory identified by Lemaire and Kowalkowski (1981) as the plasmapause. All plasma holes formed anywhere in the magnetosphere will collect and form a trough at this trajectory along which the gravitational force is, on the average, balanced by the "centrifugal force". The large plasma density enhancement formed beyond this trough becomes a detached plasma element which ultimately moves away from the Earth because of the outward directed "centrifugal force".

To test this model of plasmapause based on plasma interchange motion, we have taken advantage of the availability of a 3-day sequence of whistler and satellite data covering the magnetic storm of July 29, 1977, to compare theoretical predictions of the time-varying position of the plasmapause with its observed location.

This IMS event was the topic of a Coordinated Data Analysis Workshop in October 1979. It was chosen for different reasons, the most important of which was that several substorms occurred on that day following a very quiet period (Manka et al., 1982), and that the magnetopause moved inward to a near-record minimum nose distance of 6.2 R_E after the arrival of an interplanetary shock at 0027 UT (Knott et al., 1982). Later in the day, the interplanetary magnetic field turned northward, the magnetosphere became quiet, and the polar cap collapsed to a very small area. July 29, 1977, was a day with very strong activity and very rapid changes of magnetospheric boundaries, in particular of the plasmapause for which we have a relatively large number of good experimental data.

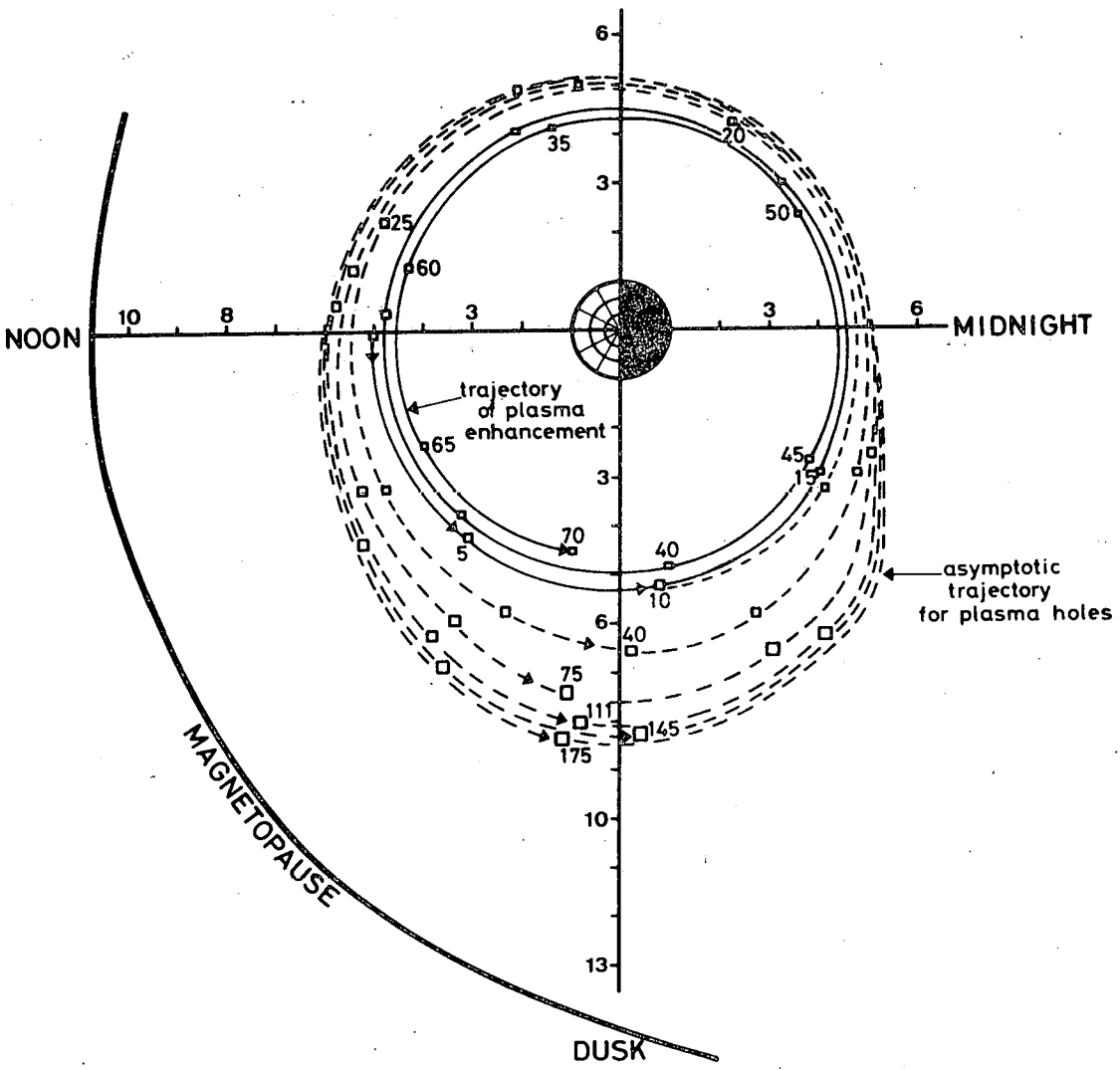

Fig. 1.- Equatorial drift path of a plasma density enhancement (solid curve) and of a plasma hole (dashed curve) whose density are respectively 20% larger and 20% smaller than the background density. The asymptotic trajectory of all plasma holes determine the position of the equatorial plasmapause (from Lemaire and Kowalkowski, 1981).

2. THEORETICAL STUDY OF THE PLASMAPAUSE EVOLUTION

2.1. Time dependent electric field models

According to the two alternative theories mentioned above, the curves defining the plasmapause should coincide with a sharp drop in thermal plasma concentration, but only if the global electric field pattern has remained stationary for at least one day, which is the time required for a plasma element to be convected all the way round the Earth.

Unfortunately, the electric field distribution is seldom, if ever, stationary for a long period of time; the outer plasmasphere is usually in a dynamic state of recovery (Corcuff et al., 1972; Carpenter and Park, 1973). Global time dependent electric field distributions are difficult to determine from spacecraft observations alone, or even from ground based whistler observations presently available. But there is already plenty of experimental evidence that, at the onset of substorms, the dawn-dusk component of the large scale magnetospheric electric field is strongly enhanced. It has become a standard procedure to correlate this enhancement in the dawn-dusk component of the geoelectric field with the increase in the geomagnetic activity as measured by the index Kp (Grebowsky et al, 1974; Chen et al., 1975). Although the three-hour index Kp may not be the best choice (Spiro et al., 1981), here we have followed this standard procedure, and have assumed that the global geoelectric field is uniquely determined by the instantaneous value of Kp.

Several empirical relations between the electric field strength and the magnetic activity index Kp (or Km) have been deduced from different types of measurements. A comparative study by Berchem and Etcheto (1981) shows that the relationship established by Carpenter and Park (1973) :

$$Lpp = 5.7 - 0.47\ Kp \qquad (1)$$

is quite representative in determining the equatorial plasmapause position Lpp in the post-midnight sector as a function of Kp.

We have introduced this relation in the two following electric field models which have been used to simulate the motions of the equatorial plasmapause during the substorm events of July 29, 1977. In order to smooth out the sharp discontinuities existing in the three-hour Kp values as a function of Universal Time, we have constructed a slightly different index whose values are shown by a solid line in figure 2; the arrow marks the instant of the storm sudden commencement.

a) A time dependent electric field distribution derived from the Volland-Stern model

Volland (1973) and Stern (1974, 1975) have introduced a semi-empirical geoelectric field model which has one more free parameter than the original model of Kavanagh et al. (1968). In a corotating frame of reference, their convection electric field can be derived from the potential (see for instance Maynard and Chen, 1975; Ejiri et al., 1978) :

$$\phi = AR^{\gamma} \sin \varphi \qquad (2)$$

where R is the geocentric distance in Earth radii, the geomagnetic longitude, A a coefficient related to the intensity of the electric field and γ a parameter which, according to Volland and Stern, can best be set equal to 2. Ejiri et al. (1978) found that this steady state Volland-Stern electric field appears to predict both the plasmapause positions

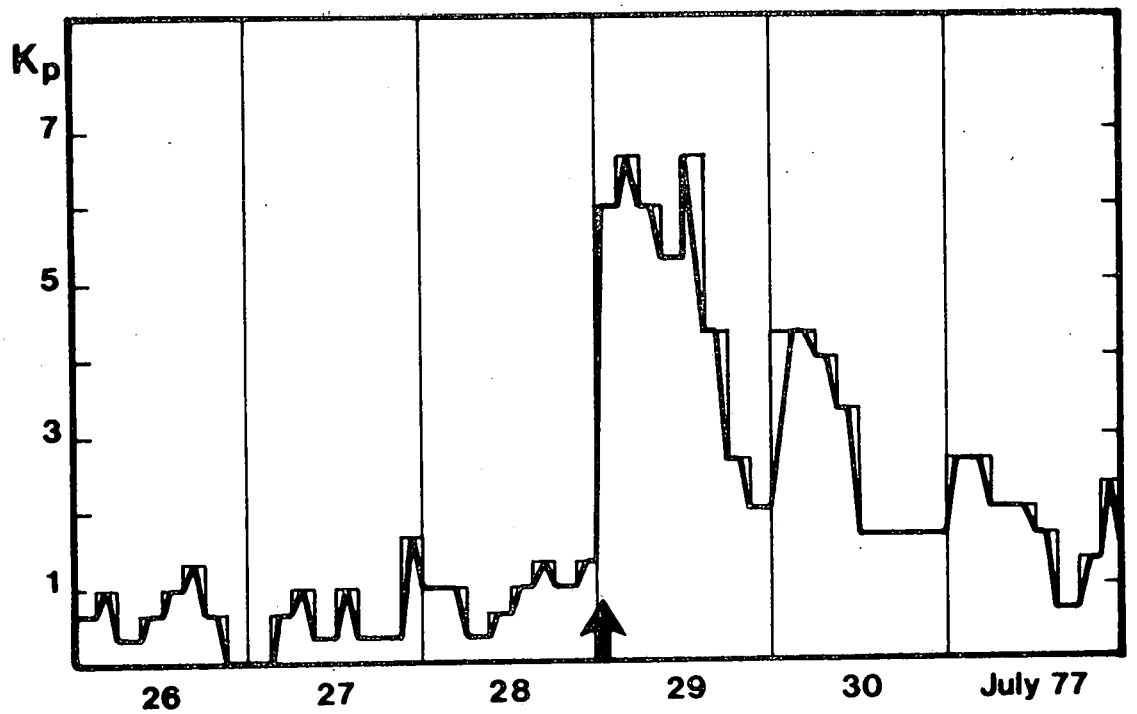

Fig. 2.- Kp index for the period July 26-31, 1977. The thicker line shows the actual variation of the index adopted in our model calculation. The arrow marks the instant of the SSC.

and the energetic particle penetrations deduced from Explorer 45 observations much better than the uniform dawn-dusk electric field which corresponds to $\gamma = 1$. Furthermore, Maynard and Chen (1975) succeeded in interpreting the locations of the plasmapause, and the isolated cold plasma regions observed with Explorer 45, by using the same model, with $\gamma = 2$, and expressing A as a function of Kp.

If the corotation electric field is superimposed on this convection field, the resulting potential is given by :

$$\Phi_t(kV) \cong - \frac{92}{R} + AR^2 \sin \varphi \qquad (3)$$

This conventional electric potential distribution has a stagnation point, and the geocentric distance at midnight (00 MLT) of the last closed equipotential passing through this dusk stagnation point is given by :

$$R_{00} = \frac{2.389}{[A(kV/R_E^2)]^{1/3}} \qquad (4)$$

In the framework of the MHD theory mentioned above, R_{00} corresponds to the plasmapause position L_{pp}. It follows then from (1) and (4) that

$$A(kV/R_E^2) = \frac{0.0736}{(1 - 0.0825\ K_p)^3} \qquad (5)$$

b) A time dependent electric field distribution derived from McIlwain's E3H model

McIlwain (1972, 1974) deduced the E3H empirical model from ATS-5 particle drift observations near geostationary orbit. In contrast to the Volland-Stern model, which has only two adjustable parameters (eq. 2), the E3H electric convection potential is given by :

$$\phi(kV) = 10\text{-}92\ (B/31000)^{1/3}$$

$$+ \sum_{i=1}^{6} \sum_{j=1}^{20} \zeta_{ij} \exp \left\{ - a_i (B - B_i)^2 - b_j\ (1 - \cos\ (\varphi\ - \varphi_j)) \right\} \qquad (6)$$

where the 120 coefficients ζ_{ij} and the other parameters B_i, b_j, a_i and φ_j have been determined by McIlwain for steady geomagnetic activity and for Kp between 1 and 2. In addition to a large dawn-dusk electric field component, this model contains an enhanced radial electric field in the post-midnight sector. The series of 6 x 20 terms in the right hand side of (6) are weighted gaussians centred at a grid of points located at 20 different local time angles (φ_j) and along 6 different B_i-shells.

Unlike the Volland-Stern model, this geoelectric field distribution has no stagnation point singularity within the limits of the magnetosphere.

To obtain better correspondence with Kp values outside the range Kp = 1-2, McIlwain (1974) suggested introducing a scale factor f such that a family of different electric field models can be derived by the conversion :

$$B_i' = \frac{B_i}{f^3} \; ; \qquad a_i' = a_i \, f^6 \; ; \qquad \zeta_{ij}' = \frac{\zeta_{ij}}{f} \qquad (7)$$

The amplitudes ζ_{ij}' of the convection electric field components increase linearly when f decreases, but the value of the product $a_i' B_i'^2$ is independent of f.

It might have been preferable to introduce different scale factors f_{ij} for each of the local time sectors centred around $_j$, and for each interval of radial distance where the equatorial magnetic field is equal to B_i. Unfortunately, without direct global measurements, such a detailed description of the magnetospheric electric field distribution is still beyond our grasp. For the time being, force of circumstances leads us to make simple assumptions about the f_{ij}'s and about their dependence on the geomagnetic activity.

The simplest assumption is then to consider that all f_{ij}'s are equal to each other and that their common value (f) is an analytic function of the three-hour geomagnetic index Kp. Note that the Volland-Stern time dependent electric field described above is also based on such a simple assumption.

The following relation between f and Kp :

$$f = 2.55 - (1.85 + 0.403 \, Kp)^{1/2} \qquad (8)$$

has been obtained in an empirical manner, in order to fit the theoretical plasmapause positions in the post-midnight sector to those given by the relation (1) from Carpenter and Park. Following the method described by Lemaire (1976), the positions of the asymptotic trajectories of plasma holes have been determined for different values of f. The corresponding

plasmapause positions at 01 MLT were then compared with Lpp, given by eq. (1), so as to obtain the relationship (8) between the scale factor f and Kp.

The question whether this empirical time dependent electric field model derived from McIlwain's stationary E-field model is or is not a satisfactory approximation of the actual global geoelectric field during the substorm of July 29, 1977, will be discussed below where the theoretical calculations are compared with the observed plasmapause positions.

2.2. Description of the theoretical model calculations

In all our calculations we have assumed that the theoretical position of the plasmapause boundary coincides at any instant of time with the trajectory of plasma density holes, as suggested by Lemaire and Kowalkowsky (1981). Plasma holes with an initial density 20% of the background density have been considered and released successively at half-hour intervals at a distance of 5 R_E in the 18 MLT sector. In fact, the final trajectory depends very little on the coordinates of the point where the plasma holes are initially released, at least for $t >> t_o$, where t_o is the initial time of integration. Consequently, the mechaniscm of plasma interchange motion leads to a plasmapause position which is independent of t_o.

The interchange velocity $\underline{u}$ has been calculated with the latitudinal and local time distribution of the integrated Pedersen conductivity given by Gurevich et al., (1976), a model which is K_p - dependent.

The convection velocity $\underline{V}$ has been determined using the two time dependent electric field distributions described in the previous section and derived successively from the Volland-Stern (V-S) model

and from McIlwain's E3H model. A dipolar magnetic field has been assumed in the first case, while the magnetic field model M2, introduced by McIlwain (1974), has been adopted in the second case.

The different panels of figure 3 show, for example, the asymptotic trajectories obtained with the V-S model (figs. 3a, 3b and 3c) and with the E3H model (figs. 3d, 3e and 3f), successively 48, 60 and 72 jours after the initial time of integration t_o = 00 UT on July 27, 1977. These trajectories correspond to the outer edge of the plasmapause respectively at 00 UT and 12 UT on July 29 and at 00 UT on July 30.

It is from a series of such figures that we have been able to determine the outer edge of the equatorial plasmapause position as a function of Universal Time in each local time sector, from 12 UT on July 28 until 24 UT on July 31, 1977. The results for the sectors 00-01, 06-07, 09-10, 12-13, 15-16 and 18-19 MLT are shown in figures 5 and 6, where the curves represent the theoretical plasmapause position as calculated using the time dependent E-field distributions derived from the V-S model (on the left hand side) and from the E3H model (on the right hand side).

The figure 3e shows that, at 12 UT on July 29, 12 hours after the SSC, plasma holes have reached the magnetopause in the afternoon sector where they are lost from the magnetosphere. Such drifts explain the gaps which appear in the theoretical curves drawn in figure 6.

3. DESCRIPTION OF EXPERIMENTAL DATA

3.1. Whistler data

The various circles on the panels of figures 5 and 6 show the results deduced from the analysis of whistlers propagated near the

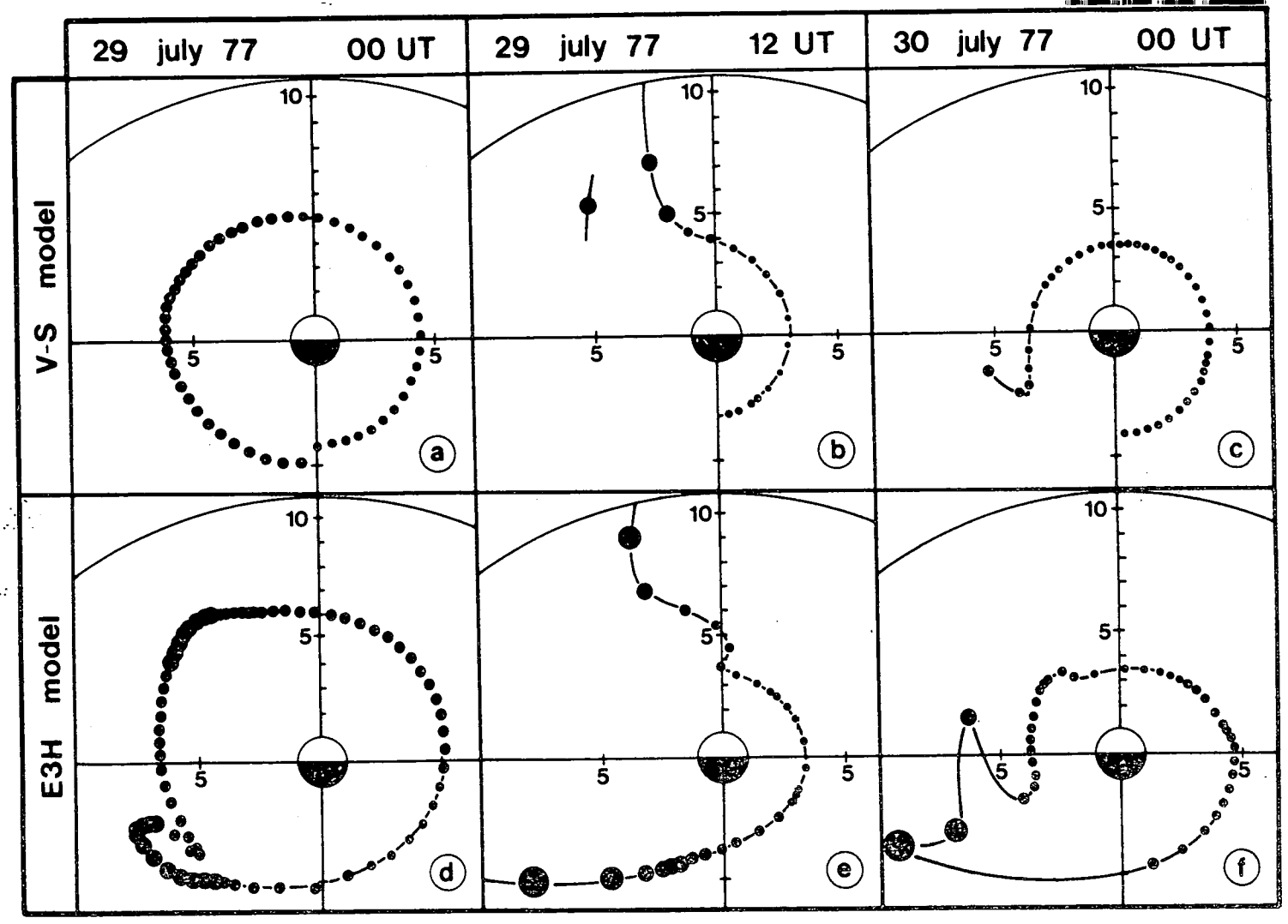

Fig. 3.- Equatorial boundaries of the plasmasphere obtained successively at 00 UT and 12 UT on July 29 and at 00 UT on July 30, 1977, with the time dependent electric field distributions derived from Volland-Stern's model (three upper panels) and from McIlwain's E3H model (three lower panels). The model calculations take into account the effect of plasma interchange motion ($u \neq 0$) and the outer edge of the plasmapause coincides with the asymptotic trajectory of plasma density holes which are successively released in the dusk sector.

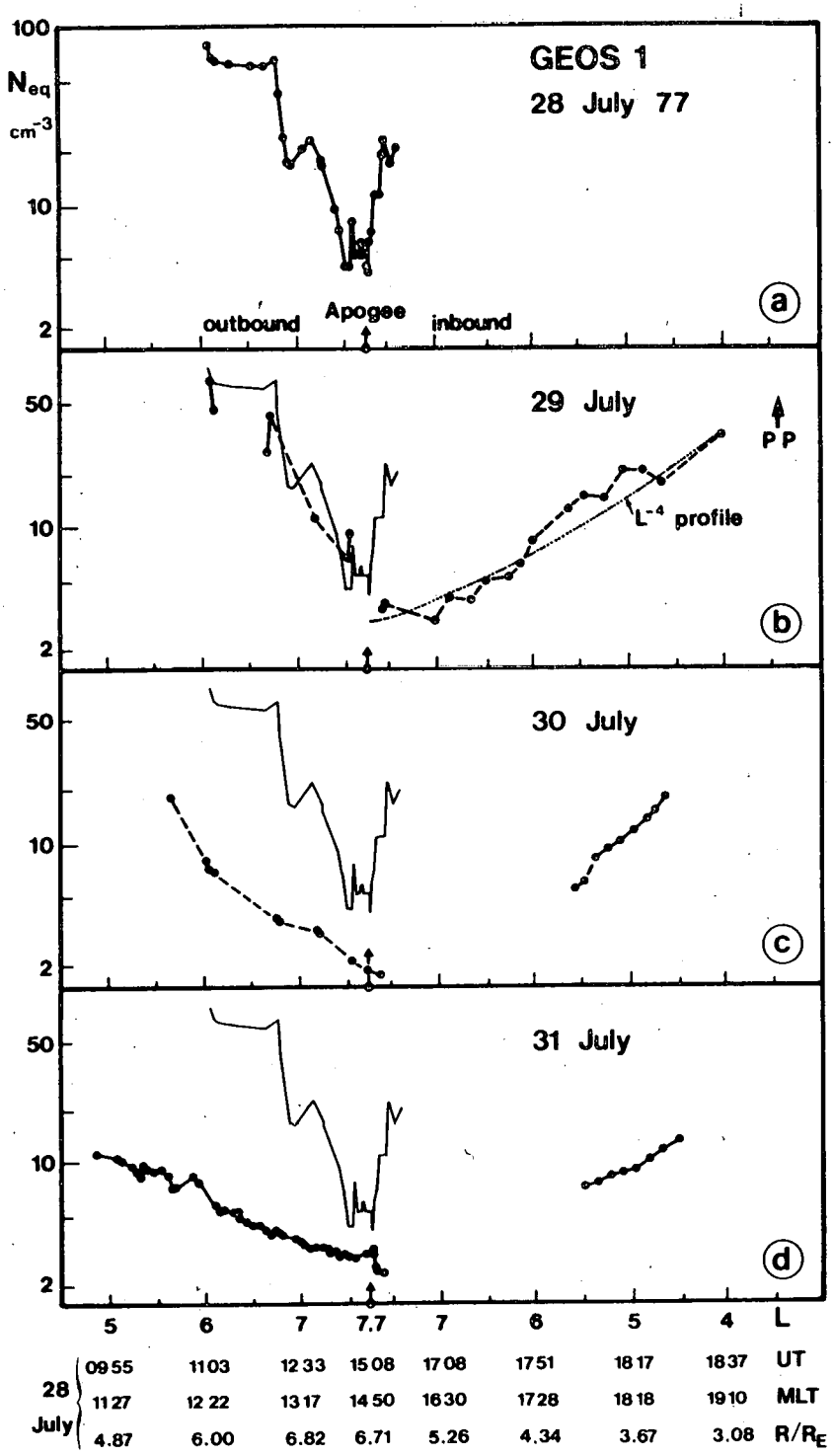

Fig. 4.- Equatorial density profiles (N_{eq}) in the afternoon-dusk sector deduced from GEOS-1 relaxation sounder data (exp. S.301) for the four last days of July 1977. The density profile of July 28, corresponding to the quiet day preceding the magnetic storm of July 29, is reproduced in each panel for comparison. The dotted parts of the profiles are smoothed interpolations when data are missing. PP refers to the plasmapause position supplied by the electric field double probe experiment on GEOS-1.

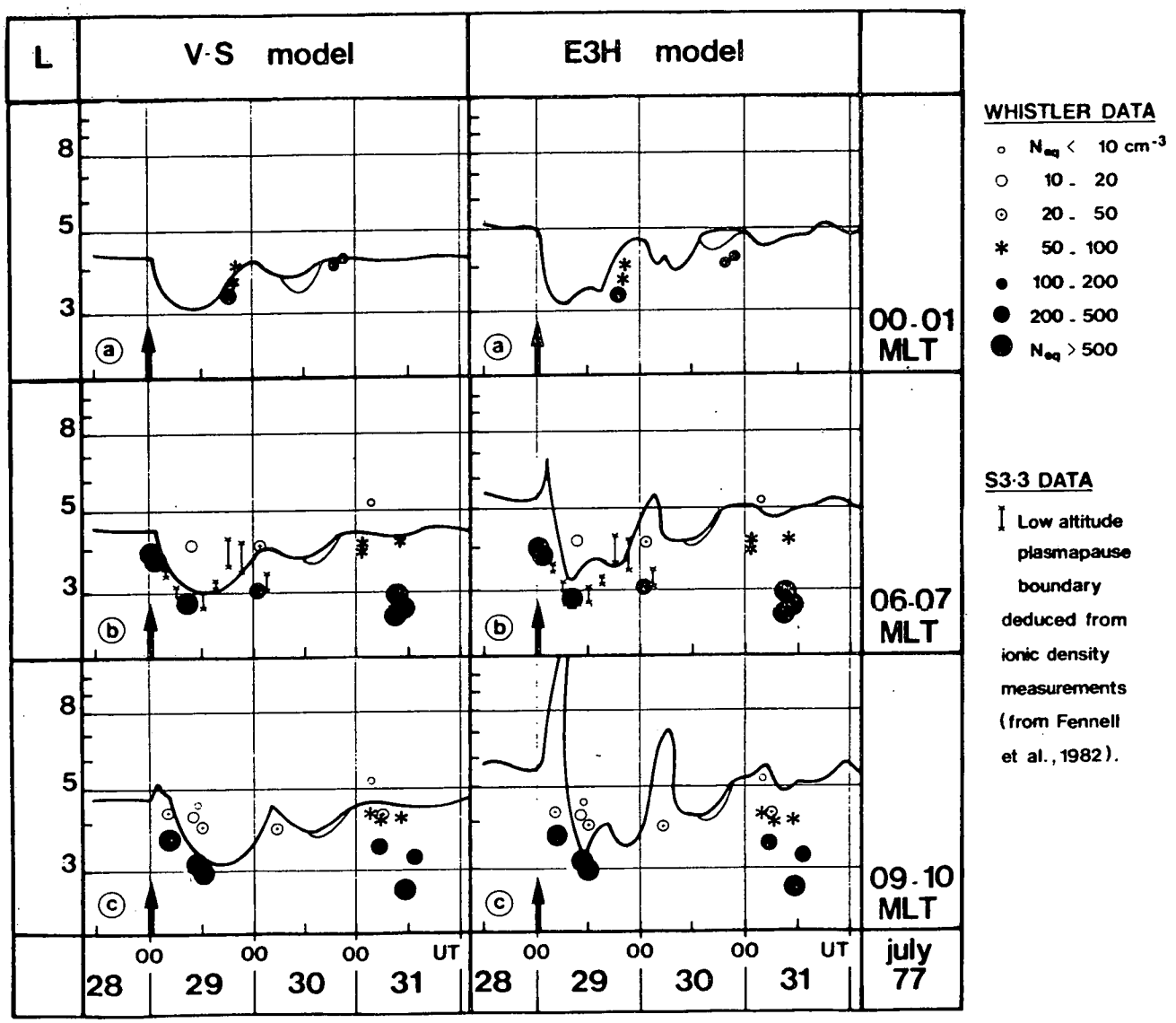

Fig. 5.- Radial distances of the equatorial plasmapause in different local time sectors versus universal time, between 12 UT on July 28 and 24 UT on July 31, 1977. The time dependent Volland-Stern's (on the left hand side) and McIlwain's E3H (on the right hand side) electric field distributions have been used in these model calculations which take into account the effect of plasma interchange motion. The different symbols show the results deduced from S3-3, GEOS-1 and whistler observations; their type and size indicate the order of magnitude of the equatorial electron density according to the scale on the right hand side. Panels a, b and c correspond to the 00-01, 06-07 and 09-10 magnetic local time sectors respectively.

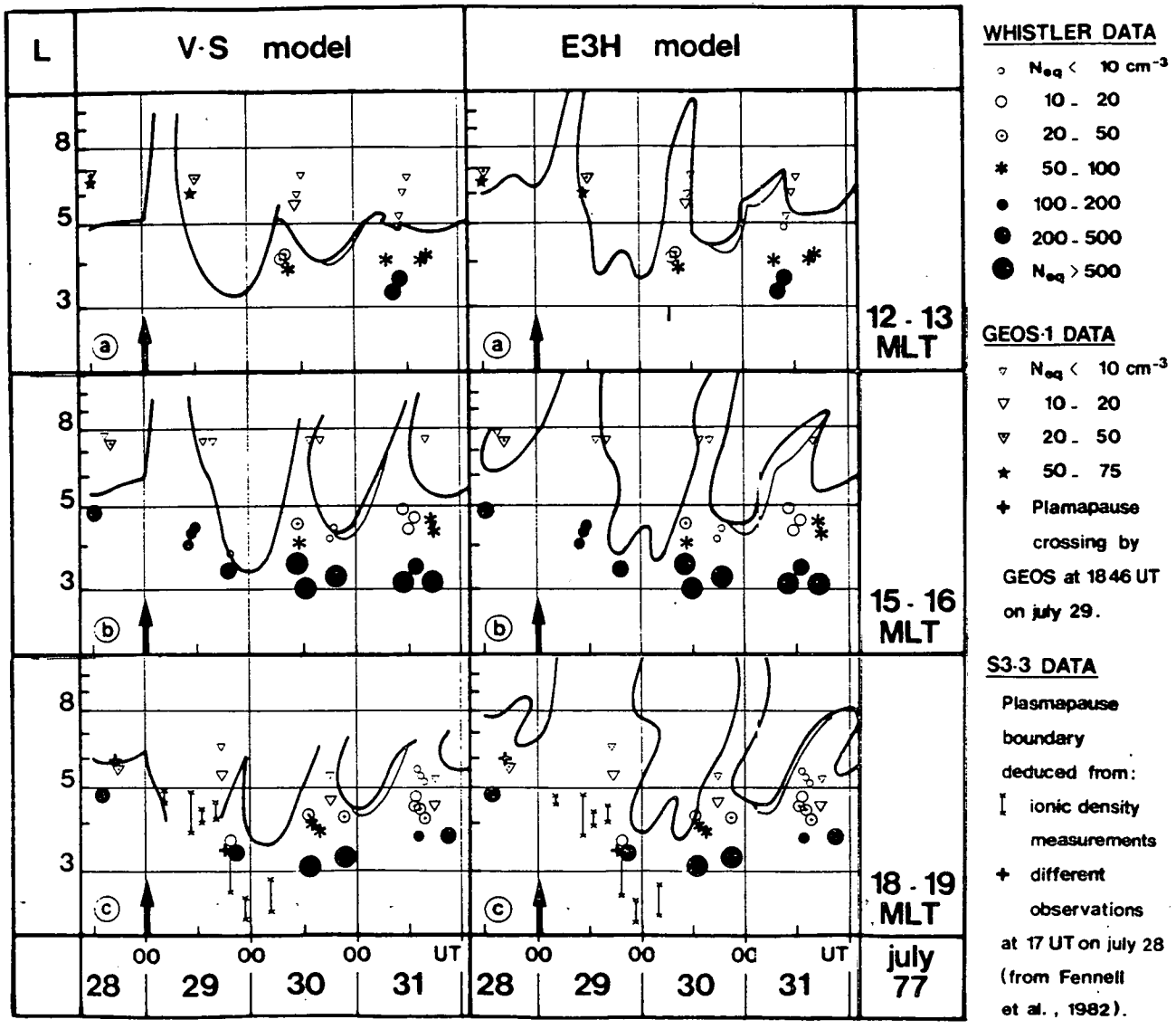

Fig. 6.- The same as in figure 5, but for other magnetic local time sectors : 12-13 MLT (a), 15-16 MLT (b) and 18-19 MLT (c).

plasmapause and recorded at Kerguelen (L = 3.7) and General Belgrano (L = 4.5) in Antarctica. Their ordinates represent the L-values of the whistler paths; their type and size indicate, according to the scale on the right hand side, the order of magnitude of the equatorial electron density. Solid circles correspond to the inner dense plasmasphere, and open circles to the tenuous region beyond the plasmapause; dots inside open circles and stars correspond to the plasmapause boundary or to expanding plasmasphere regions that have relatively low densities or that are in the process of refilling with cold ionospheric plasma.

Whistlers have been analyzed by means of Corcuff's method (1977). Equatorial electron densities and L-values of whistler ducts have been determined using a diffusive equilibrium model for all densities greater than 100 cm^{-3} (corresponding to the interior of the plasmasphere). For equatorial densities less than 100 cm^{-3}, we have used an hybrid model (Corcuff and Corcuff, 1982) with a R^{-4} density distribution in the equatorial region up to 30°, and a diffusive equilibrium distribution at higher latitudes down to an altitude of 1000 km.

3.2. GEOS-1 and S3-3 data

The small triangles on figure 6 illustrate, in a similar way, the values of the equatorial electron density deduced from in-situ measurements made by means of the relaxation sounder flown in the GEOS-1 satellite (Etcheto and Bloch, 1978). Because of experimental and orbital limitations, only densities below 75 cm^{-3}, measured between 4 and 7.5 R_E, are available from GEOS-1 data. Furthermore, in July 1977, the satellite apogee was located in the afternoon sector; therefore GEOS-1 data are shown only in figures 6a, 6b and 6c corresponding to the noon, afternoon and dusk local time sectors respectively.

On the inbound part of its orbit, the geocentric distance R (in Earth radii) of GEOS becomes distinctly lower than the L-value of the field line passing through the position of the satellite, as indicated by the abscissa scales in figure 4. Consequently, the measured density N_e is greater than the corresponding equatorial density N_{eq} at the top of the field line (Corcuff and Corcuff, 1982). The geomagnetic latitude of GEOS being always less than 30° and the measured electron density being always lower than 75 cm^{-3}, we have deduced the N_{eq} values from the relation :

$$N_{eq} = N_e \, (R/L)^4 \qquad (9)$$

assuming a R^{-4} density distribution along the field line in the equatorial region up to 30°, as in the analysis of whistlers that have propagated outside the plasmapause (see section 3.1).

Figure 4 shows the density profiles thus obtained for the period July 28-31, 1977, plotted on a linear L scale. The July 28 profile, which corresponds to the quiet day preceding the magnetic storm of July 29, is superimposed on each of other profiles for the sake of comparison. Its outbound and inbound parts exhibit a sharp plasma depletion, respectively near 1215 and 1630 UT, showing a plasmapause crossing at high L-values near 6.8 and below 7.5 in the afternoon sector. On July 29, a relatively dense zone of plasma is still seen up to 1230 UT as previously reported and interpreted by Etcheto and Bloch (1978) who studied density profiles measured between July 25 and July 29, 1977. But after having reached its apogee, GEOS stays outside the plasmasphere till at least 1830 UT or L = 4; electron density measurements based on electric double probe data show that the dusk plasmapause crossing occurs near 1846 UT or L = 3.4 (see Fennell et al., 1982).

The density profiles of July 30 and 31 are typical of a magnetically disturbed period. The density remains low during the two passes and the satellite was lost by the tracking station before encountering the plasmapause and reentering the plasmasphere. These observations are consistent with previous measurements showing that, during a magnetically disturbed period, the plasmapause is formed closer to the Earth.

Finally, in this study we have also used the estimates of the plasmapause boundary deduced by Fennell et al. (1982) from ionic density measurements made in the polar satellite S3-3, between 1000 and 4000 km altitude, near dawn and dusk. The corresponding results are indicated by vertical bars in figures 5 and 6; the length of some bars is relatively great because the density data on July 29 often show a very slow variation with invariant latitude and have regions of elevated ($\gtrsim$ 100 ions cm^{-3}) density extending over 3-6°.

In figure 6c, the cross at 17 UT on July 28 locates the low-altitude plasmapause boundary obtained from different S3-3 observations and the cross at 1846 UT on July 29 corresponds to the plasmapause crossing by GEOS. It is worthwhile to note the good agreement between the dusk plasmapause positions deduced from knee-whistlers ($3.4 < L_{pp} < 3.6$ at 1955 UT), GEOS-1 ($L_{pp} = 3,4$ at 1846 UT) and S3-3 ($2.6 < L_{pp} < 3.5$ at 1930 UT) data.

4. COMPARISON OF MODEL PREDICTIONS AND EXPERIMENTAL RESULTS

a) From figures 5 and 6, it can be seen that according to the two different simulations presented, the plasmasphere experiences large radial displacements in all local time sectors as a consequence of the intense substorm activity during the first 15 hours of July 29. However, the directions of these deformations and the response time of

the plasmasphere depend very much on the magnetic local time and on the assumed geoelectric field distribution.

In the post-midnight local time sector (fig. 5a), there is an immediate compression of the plasmasphere when K_p increases : the plasmapause moves, in less than six hours, from an initial position beyond 4 R_E to a minimum position near 3 R_E. This is consistent with current ideas about plasmapause dynamics based on experimental evidence (Chappell et al., 1970a; Carpenter and Park, 1973; Corcuff, 1975).

At the same time there is an outward motion of the plasmapause in the noon local time sector immediately after the SSC indicated by an arrow at 00 UT on July 29 (fig. 6a). The relatively high values of the equatorial electron densities ($N_{eq} \sim 65$ and 45 cm^{-3}) measured by GEOS-1 in this local time sector, respectively at about 11 and 12 UT on July 29 (see figure 4b, between 6 and 6.5 R_E), confirm the radial expansion of the dayside plasmasphere predicted by both model calculations.

In both simulations the inward displacement of the plasmapause, which immediately follows the SSC in the nightside, appears in the dayside with a time delay which increases linearly with magnetic local time. The experimental data confirm these theoretical results, especially in the dawn sector (fig. 5b) where the data from the S3-3 satellite are in good agreement with those deduced from whistlers and from GEOS-1 observations. In this sector the plasmapause moves closer to the Earth with a short time delay after the SSC; it reaches a minimum radial distance of 3 R_E around 12 UT on July 29 in good agreement with both model calculations.

b) According to the experimental data in figure 6c the plasmapause also moves closer to the Earth in the dusk just after the SSC :

two distinct successive inward motions can be identified. The first inward motion brings the duskside plasmapause from a pre-SSC position close to 6 R_E to a post SSC position at 4.8 R_E. This inward motion is rather well simulated by the calculations based on the Volland-Stern model (fig. 6c, left hand side panel) for which the stagnation point moves closer to the Earth when the dawn-dusk E-field component increases as K_p is enhanced. The outer part of the duskside plasmasphere is then ripped off by an enhanced westward convection velocity.

A rather different evolution of the plasmapause position is shown in the right hand side panel of figure 6c obtained with the time dependent E3H model described in section 2.1b. According to this model, the duskside plasmasphere and its outer edge expand radially up to the magnetopause beyond 10 R_E immediately after the onset of the SSC. As a consequence, the equatorial density distribution in the dusk sector is reduced. Also possibly, as a result of this radial expansion, another "knee" can be formed closer to the Earth at the boundary between the inner dense corotating part of the plasmasphere and an outer expanded one. The actual location of that "knee" has not, however, been determined numerically in this paper.

It can already be concluded, therefore, that in the dusk local time sector the position of the outer edge of the plasmasphere obtained with the time dependent model of Volland-Stern differs drastically from that calculated with the E3H model. In the former case this boundary moves closer to the Earth and the sheared plasmasphere should terminate rather steeply, while in the latter case the duskside plasmasphere is widely expanded after the onset of the SSC. At a first glance, the experimental data shown in figures 6c between 00 UT and 24 UT on July 29 seem to support better the former E-field model more than the latter one. However these observations can equally well be used in support of the E3H model calculations and can be interpreted as the inner edge of an expanded plasmasphere region. Indeed, as

indicated by the inbound part of the July 29 profile in figure 4b, the density profile in the afternoon and dusk sectors between L = 7.7 and L = 4 resembles the L^{-4} shape; this is typical of the expanded plasmaspheres which are often observed in these local time sectors (Chappell et al., 1970b; Berchem and Etcheto, 1981; Décréau et al., 1982; Corcuff and Corcuff 1982). The relatively low values of N_{eq} measured in this region show that this expanded part of the plasmasphere is partly depleted, as indeed predicted from the E3H model calculations. A clear cut answer to these two alternatives scenario would required, however, detailed multistation and coordinated observations including plasma bulk velocity measurements.

c) A second large amplitude inward displacement of the dusk-side plasmapause starts at 18 UT on July 29, i.e. almost 18 hours after the SSC; as already discussed above this delay corresponds approximatively to the time required for a plasma element to be convected from the midnight to the dusk sectors. The observed geocentric distance of the plasmapause decreases then in less than 6 hours from 4.8 R_E to 2.5 R_E.

These experimental results support those found by Décréau et al. (1982) and Décréau (1983) who studied the dynamical response of the thermal plasma parameters measured by GEOS-1 and GEOS-2 as a function of the level of geomagnetic activity. These observations are in favour of the mechanism of formation of the plasmapause proposed by Lemaire (1975), according to which there is a "peeling off" and an earthward motion of the plasmasphere near midnight when the substorm activity increases. The peeling off mechanism by interchange instability during periods of enhanced penetration of convection electric fields in the inner nightside magnetosphere leads to the formation of a new plasmapause closer to the Earth in the post midnight local time sector. This new boundary then corotates toward the dayside; the time delay

after which the inward motion is observed in the dayside is approximately proportional to the local time corresponding to the corotation propagation time.

According to our two model simulations, it takes almost 18-24 hours for the new plasmapause formed near midnight to "corotate" around the Earth and to reach the duskside. The minimum plasmapause position shown in figures 6c near 00 UT on July 30 is a direct consequence of this "corotation" effect. The other two minima in the theoretical duskside plasmapause positions, seen respectively at ∿ 09 UT on July 30 and at ∿ 03 UT on July 31, correspond to the plasmapauses formed near midnight during the two enhancements of geomagnetic activity at 12 UT on July 29 and at 00 UT on July 30 (fig. 2).

Consequently, the theory for the formation of a new plasmapause at each substorm enhancement - on which both model calculations are based - fits the observed corotation time delays observed by Geos 1 and 2 as well as those reported by Chappell et al. (1971) and deduced from OGO 5 observations. The agreement with the observations clearly indicates that the plasmapause "peeling off" takes place near midnight local time, and, not near dusk as a result of shearing near the stagnation point in the case of a Volland-Stern model.

d) At 06 and 09 MLT (figs. 5b and 5c), and immediately after the onset of the substorm events of July 29 and 30, there is a rapid and short duration increase in the equatorial distance of the plasmapause in the case of the E3H model. The experimental data do not indicate, however, such a radial expansion of the plasmasphere as early as 06 MLT. They show, respectively at 04 and 05 UT, that the plasmapause is located at geocentric distances close to 4 R_E, and almost coincident with the positions predicted by the Volland-Stern model; on the contrary with the time dependent E3H model, the corresponding plasmapause distances are significantly greater.

This is another major difference between the two E-field models. While in the Volland-Stern model, only the dawn-dusk component of the electric field is enhanced when K_p increases, in the E3H model there is an additional enhancement of the eastward component in the morning and dayside sectors from 06 MLT to 18 MLT. Since this result from the E3H model calculation is not well supported by the experimental results at 06 and 09 MLT, it must be concluded that some of the assumptions made in section 2.1b in the derivation of the time dependent E-field model from McIlwain's stationary E3H electric field distribution, were not appropriate. It is probable, indeed, that the scale factors, f_{ij}, of the different electric field components in the dawn and dayside sectors ought not to be the same as in the postmidnight sector where eq. (8) fits the observations rather well. Other assumptions will be tried in the future to improve the E3H time dependent magnetospheric E-field model in the dawn local time sector as well as anywhere else, where such improvement will appear to be necessary.

The fairly good fits obtained with the Volland-Stern time dependent electric field model described in Section 2.1a indicates that this simple model is a rather satisfactory first approximation of the actual E-field distribution in the dawn sector of the magnetosphere.

e) The solid dots corresponding to observed densities greater than 100 cm^{-3} are all located earthward of the theoretical plasmapause positions in both simulations illustrated in figs. 5 and 6. None of these points corresponding to plasmaspheric high densities falls beyond the calculated outer edge of the plasmapause.

Furthermore, all intermediate plasma densities ($20 < N_{eq} < 100$ cm^{-3}; indicates by solid stars in figs. 5 and 6) are also observed during the recovery phase of July 30 and 31, inside the positions of the plasmapause calculated by taking into account plasma interchange motion.

However, when interchange motion is neglected-or inhibited by setting $\Sigma_p = \infty$ in the numerical calculations- we have obtained the plasmapause positions which are shown in the right hand side panels of fig. 7a, b and c for Volland-Stern's field model.

The intermediate plasma density data, also represented by solid stars in fig. 7, correspond to expanded afternoon plasmaspheric regions or to post-dawn magnetic flux tubes in the process of refilling. These flux tubes are expected to be located inside the outer edge of the plasmapause as it is the case in the left hand side panels of fig. 7 where realistic values for the integrated Pedersen conductivity (Σ_p) have been used to compute the maximum interchange velocity. In the right hand side panels of fig. 7, however, the solid stars are located outside the plasmapause which is determined in this instance by using the classical MHD convection theory : i.e. without interchange motion. This comparison indicates that, after major substorm events the positions of the plasmapause calculated with interchange motion are much more consistent with the observations than those obtained when this physical mechanism is neglected; indeed in the latter case the plasmapause remains at too low L-values, after a large geomagnetic perturbation. On the contrary, according to the theory proposed by Lemaire (1975), the plasmapause reforms itself rapidly at larger radial distances during recovery phases as confirmed by all available observations.

5. SUMMARY AND CONCLUSIONS

Two different types of time dependent electric field distributions have been used to illustrate the formation of a plasmapause when the plasma interchange mechanism is taken into account : the first type of E-field distribution is derived in section 2.1a from the Volland-Stern model and has a stagnation point at 1800 MLT; the second one is derived in section 2.1b from McIlwain's stationary E3H model.

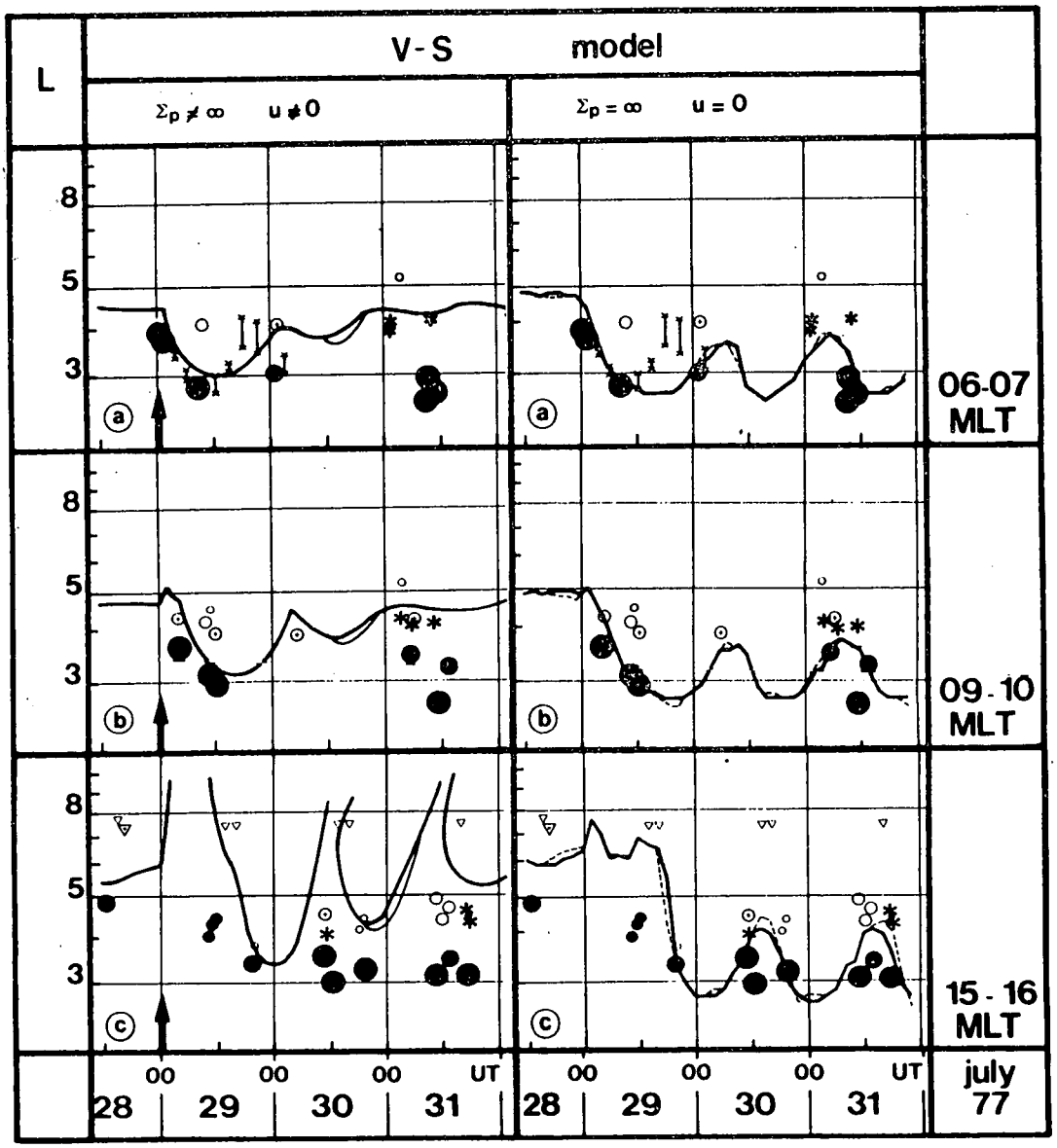

Fig. 7.- Radial distances of the outer edge of plasmapause region in three different local time sectors as a function of Universal Time from July 28 to July 31, 1977. The time dependent Volland-Stern electric field distribution has been used in all these simulations. In the left hand side panels realistic values for the integrated Pedersen conductivity have been used to calculate the plasma interchange velocity. In the right hand side panels plasma interchange velocity is assumed to be equal to zero as in the MHD theory for the formation of the plasmapause. The various symbols have the same meanings as in figure 6.

The time dependent plasmapause positions obtained for realistic values of the integrated Pedersen conductivity (i.e. for non-zero values of the interchange velocity u) are shown in figures 5 and 6 for a period of three and a half days including the substorm events of July 29 and July 30, 1977. Those corresponding to the Volland-Stern model are given on the left hand side; those corresponding to the E3H model are shown on the right hand side panels.

Large amplitude deformations of the calculated plasmapause occur after periods of enhanced geomagnetic activity. Dawn-dusk as well as noon-midnight asymmetries are found in the positions of the plasmapause for both E-field models (compare for example figures 5c and 6c as well as 5a and 6a). These asymmetries in the shape of the plasmasphere are confirmed by our observations as well as by previous experimental data (Carpenter, 1966; Gringauz and Bezrukikh, 1976; Higel and Wu Lei, 1984).

The inward and outward motions of the midnight and post-midnight plasmapause are qualitatively similar for both E-field model (compare the two panels of figure 5a). But this is not surprising since the time dependent electric field models have both been tailored to fit Carpenter and Park's (1973) relation in this particular local time sector (eq. 1).

The largest deformations of the plasmapause are however obtained in the afternoon and dusk local time sectors for both E-field models (see the left and right hand side panels of figures 6b and 6c). It is evident that there are here large discrepancies between both model predictions. The reason is that the maximum interchange velocity (u) is small compared to the total drift velocity (V + u). This is especially the case in the dayside region where the integrated Pedersen conductivity is largest. Therefore, large amplitude and fast deformations of a plasma-pause boundary are direct consequences of temporal variations of the

large convection velocity (V) which is very different in both E-field models, specially in the afternoon and dusk sectors.

Although the mechanism of interchange motion is slow compared to magnetospheric convection, it plays however a key role in peeling off the plasmasphere in the post-midnight sector and in forming a new plasmapause where the gravitational force becomes smaller than the "centrifugal" or inertial forces. The new plasmapause formed in the post-midnight sector, where the interchange instability has a maximum growth rate, is observed later in the dayside local time sectors, after a time delay nearly proportional to the local time. These model predictions are very well confirmed by the observations presented in this paper and by others : Chappell et al. (1971), Décreau et al (1982) and Corcuff and Corcuff (1982).

The positions of the plasmapause obtained with Volland-Stern's model and when interchange motion is not taken into account, are illustrated in the right hand side panels of fig. 7. It can be seen that the plasmapause remains then at too low L-values after a substorm. The corresponding results when interchange motion is taken into account are shown in the left hand side panels of fig. 7; these latter results fit the observations much better. Indeed, after an enhancement of K_p, the new plasmapause forms then again at larger radial distances as indicated by the observations. Consequently, the agreement between observations and plasmapause model calculations is improved when interchange motion is taken into account in the theory of formation of this surface of discontinuity.

From the intercomparison of the theoretical model calculations presented in the left and right hand side panels of fig. 6, it difficult to conclude which of both electric field models used in this study fits better the observations in the afternoon and dusk side sectors. Indeed it has been shown above that these observations can be interpreted in

two alternative way which support either one or the other time dependent E-field models described in sections 2.1a and 2.1b respectively. Multistation and coordinated observations of the plasmapause positions and bulk velocity would be needed to resolve this issue.

There is another major difference between the results obtained in both model simulations shown in figs. 5b and 5c, for 06 and 09 MLT. In the right hand side panels corresponding to the E3H model calculations, the plasmapause has a short duration radial expansion immediately after the storm sudden commencement of July 29. This radial plasmaspheric expansion is not obtained with Volland-Stern's model as early in the dawn local time sector. In the observations presented above, there is no definite indication for such a radial expansion. Consequently, the time dependent E3H model derived in section 2.1b, needs probably to be corrected in order to eliminate this bias in the dawn local time sector. To correct such bias one could for instance introduce different scale factors for all the terms in the expansion (6) and (7). Ad hoc empirical relationships between K_p and different scale factors f_{ij} can be introduced to avoid the undesired enhancement of the eastward E-field component in the 06-09 MLT sector. In principle the scale factors f_{ij} can be changed at will to fit a wide range of stationary or time dependent magnetospheric E-field distributions. Such an improvement has already been included in the E-field model used in a simulation presented on video cassette by Lemaire (1984).

A detailed study of the plasmasphere dynamics and of its deformations during selected periods of time like that considered in this article can be rather fruitful to infer the empirical electric field morphology which fits best the observations.

ACKNOWLEDGEMENTS

We wish to thank Mr. M.G. MINNIS for reading and improving the manuscript as well as Mrs. J. ETCHETO for GEOS-1 data and Mrs. P. DECREAU for her valuable critical comments. This research was supported, respectively in France and Belgium, by the Centre National de la Recherche Scientifique in the framework of the ATP "Etude Internationale de la Magnétosphère" and by the Fonds National de la Recherche Scientifique through the "Crédits aux Chercheurs".

REFERENCES

BERCHEM J., ETCHETO J., 1981. Experimental study of magnetospheric convection, Advances in Space Research, 1, 179-184.

BRICE N.M., 1967. Bulk motion in the magnetosphere, J. Geophys. Res., 72, 5193-5211.

CARPENTER D.L., 1966. Whistler studies of the plasmapause in the magnetosphere. 1. Temporal variations in the position of the knee and some evidence on plasma motions near the knee, J. Geophys. Res., 71, 693-709.

CARPENTER D.L., PARK C.G., 1973. On what ionospheric workers should know about the plasmapause-plasmasphere, Rev. Geophys. Space Phys., 11, 133-154.

CHAPPELL C.R., HARRIS K.K., SHARP, G.W., 1970a. A study of the influence of magnetic activity on the location of the plasmapause as measured by Ogo 5, J. Geophys. Res., 75, 50-56.

CHAPPELL C.R., HARRIS K.K., SHARP, G.W., 1970b. The morphology of the bulge region of the plasmasphere, J. Geophys. Res., 75, 3848-3861.

CHAPPELL, C.R., K.K. HARRIS and G.W. SHARP, 1971. The dayside of the plasmapause, J. Geophys. Res., 76, 7632-7647.

CHEN, A.J., GREBOWSKY, J.M., TAYLOR, H.A., 1975. Dynamics of mid-latitude light ion trough and plasma tails, J. Geophys. Res., 80, 968-976.

CORCUFF P., 1977. Méthodes d'analyse des sifflements électroniques : 1. Application à des sifflements théoriques, Ann. Géophys., 33, 443-454.

CORCUFF P., CORCUFF Y., CARPENTER D.L., CHAPPELL C.R., VIGNERON J., KLEIMENOVA N., 1972. La plasmasphère en période de recouvrement magnétique. Etude combinée des satellites OGO 4, OGO 5 et des sifflements reçus au sol, Ann. Géophys., 28, 670-695.

CORCUFF Y., 1975. Probing the plasmapause by whistlers, Ann. Géophys., 31, 53-78.

CORCUFF Y., CORCUFF P., 1982. Structure et dynamique de la plasmapause-plasmasphère les 6 et 14 juillet 1977 : étude à l'aide des données de sifflements reçus au sol et de données des satellites ISIS et GEOS-1, Ann. Géophys., 38, 1-24.

DECREAU P.M.E., 1983. Fonctionnement d'une sonde quadripolaire sur satellite géostationnaire (expérience GEOS). Contribution à l'étude du comportement du plasma froid au voisinage de la plasmapause équatoriale, Thèse de Doctorat, Univ. d'Orléans.

DECREAU P.M.E., BEGHIN C., PARROT M., 1982. Global characteristics of the cold plasma in the equatorial plasmapause region as deduced from the GEOS-1 mutual impedance probe, J. Geophys. Res., 87, 695-712.

EJIRI M., HOFFMAN R.A., SMITH, H., 1978. The convection electric field model for the magnetosphere based on Explorer 45 observations, J. Geophys. Res., 83, 4811-4815.

ETCHETO J., BLOCH J.J., 1978. Plasma density measurements from the GEOS-1 relaxation sounder, Space Sci. Rev., 22, 597-610.

FENNELL J.F., JOHNSON R.G., YOUNG D.T., TORBERT R.B., MOORE T.E., 1982. Plasma and electric field boundaries at high and low altitudes on July 29, 1977, J. Geophys. Res., 87, 5933-5942.

GREBOWSKY J.M., TULUNAY Y.K., CHEN A.J., 1974. Temporal variations in the dawn and dusk midlatitude trough and plasmapause position, Planet. Space Sci., 22, 1089-1099.

GRINGAUZ K.I., BEZRUKIKH V.V. 1976. Asymmetry of the Earth's plasmasphere in the direction noon-midnight from Prognoz 1 and Prognoz-2 data, J. Atmos. Terr. Phys., 38, 1071-1076.

GUREVICH A.V., KRYLOV A.L., TSEDILINA Ye., 1976. Electric fields in the Earth's magnetosphere and ionosphere, Space Sci. Rev., 19, 59-160.

HIGEL, B., WU LEI, 1984. Electron density and plasmapause characteristics at 6.6. R_E : a statistical study of the GEOS-2 relaxation sounder data, J. Geophys. Res., 89, 1583-1601.

KAVANAGH L.D., FREEMAN J.W., Jr., CHEN A.J., 1968. Plasma flow in the magnetosphere, J. Geophys. Res., 73, 5511-5519.

KNOTT K., FAIRFIELD D., KORTH A., YOUNG D.T., 1982. Observations near the magnetopause at the onset of the July 29, 1977, sudden storm commencement, J. Geophys. Res., 87, 5888-5894.

LEMAIRE J., 1974. The "Roche-Limit" of ionospheric plasma and the formation of the plasmapause, Planet. Space Sci., 22, 757-766.

LEMAIRE J., 1975. The mechanisms of formation of the plasmapause, Ann. Géophys., 31, 175-189.

LEMAIRE J., 1976. Steady state plasmapause positions deduced from McIlwain's electric field models, J. Atmos. Terr. Phys., 38, 1041-1046.

LEMAIRE J., 1984. Formation and deformation of the plasmapause during a substorm event, to be published in Proceedings of Conference on "Résultats du projet ARCAD 3 et des programmes récents en physique de la magnétosphère et de l'ionosphère", Toulouse 22-25 May, 1984 (ed. CNRS, Paris).

LEMAIRE J., KOWALKOWSKI L., 1981. The role of plasma interchange motion for the formation of a plasmapause, Planet. Space Sci., 29, 469-478.

MANKA R.H., FRITZ T.A., JOHNSON R.G., WOLF R.A., TEAGUE M.J., VETTE J.I., 1982. Overview of the IMS July 29, 1977, Magnetic storm analysis, J. Geophys. Res., 87, 5871-5880.

MAYNARD N.C., CHEN A.J. 1975. Isolated cold plasma regions : observations and their relation to possible production mechanisms, J. Geophys. Res., 80, 1009-1013.

McILWAIN C.E., 1972. Plasma convection in the vicinity of the geosynchronous orbit, in Earth Magnetospheric Processes (Ed. B.M. McCormac), pp. 268-179, D. Reidel, Dordrecht-Holland.

McILWAIN C.E., 1974. Substorm injection boundaries, in Magnetospheric Physics (Ed. B.M. McCormac), pp. 143-154, D. Reidel, Dordrecht-Holland.

NISHIDA A., 1966. Formation of plasmapause, or magnetospheric plasma knee, by the combined action of magnetospheric convection and plasma escape from the tail, J. Geophys. Res., 71, 5669-5679.

SPIRO R.W., HAREL M., WOLF R.A., REIFF P.H., 1981. Quantitative simulation of a magnetospheric substorm. 3. Plasmaspheric electric fields and evolution of the plasmapause, J. Geophys. Res., 86, 2261-2272.

STERN D.P., 1974. Models of the Earth's electric field, NASA/GSFC X, Doc. 602-74-159.

STERN D.P., 1975. The motion of a proton in the equatorial magnetosphere, J. Geophys. Res., 80, 595-599.

STERN D.P., 1977. Large-scale electric fields in the Earth's magnetosphere, Rev. Geophys. Space Phys., 15, 156-194.

VOLLAND H., 1973. A semi-empirical model of large-scale magnetospheric electric fields, J. Geophys. Res., 78, 171-180.